Research Square

Preprints are preliminary reports that have not undergone peer review.
They should not be considered conclusive, used to inform clinical practice,
or referenced by the media as validated information.

Assessment of the neutron fluence during operation of CEMHTI Cyclotron using Monte-Carlo codes - Simβ-AD study

Jean-Michel HORODYNSKI

jean-michel.horodynski@cnrs.fr

CNRS-iRSD, CNRS Physique-UAR3364

Abir HASSANI

CNRS-iRSD, CNRS Physique-UAR3364

Frédéric CHAPELLE

CNRS-iRSD, CNRS Physique-UAR3364

Nicolas ARBOR

Université de Strasbourg, CNRS, IPHC UMR7178

Djokhar BETELGUERIEV

Université de Strasbourg, CNRS, IPHC UMR7178

Lucia Victoria GARCIA GARCIA

Université de Strasbourg, CNRS, IPHC UMR7178

Stéphane HIGUERET

Université de Strasbourg, CNRS, IPHC UMR7178

Léo NOWAK

TRAD

Cédric DOSSAT

TRAD

Sébastien BOUILLON

CEMHTI, CNRS Chimie-UAR3079

David CHAULIN

CEMHTI, CNRS Chimie-UAR3079

William HATE

CEMHTI, CNRS Chimie-UAR3079

Patrice RIFARD

CEMHTI, CNRS Chimie-UAR3079

Thierry SAUVAGE

CEMHTI, CNRS Chimie-UAR3079

Research Article

Keywords: Activation, Cyclotron, Radioactive Waste Management, Particle Accelerators

Posted Date: July 7th, 2026

DOI: https://doi.org/10.21203/rs.3.rs-9706034/v1

License: This work is licensed under a Creative Commons Attribution 4.0 International License.
Read Full License

Additional Declarations: No competing interests reported.

Abstract

The main goal of the Sim*β*-AD study is to provide a methodology to assess activation of radioactive waste produced by cyclotron facilities, combining Monte-Carlo codes and active neutron detectors. These first experiments started in 2021 in the CEMHTI Cyclotron facility during the last years of operation (the accelerator was shut down in 2023) to define the neutron fluence inside the vault for the main primary beam used (protons and deuterons), comparing results from four Monte-Carlo codes (FLUKA

- MCNP6 - PHITS - RayXpert®) and results from irradiation of activation foils. Good agreements are reached with the different codes (ratio between measurements and calculations in a range of 0.5–1.5) using rather simplified models and off-line activity calculations with the FISPACT-II and a pre-version of RayActive code.

Introduction

Radioactive waste management needs accurate radiological characterization, especially *β*-only radionuclides (36Cl, 49V, 55Fe, 63Ni…) for which only destructive methods can be used to measure it (*β*-spectroscopy). Sim*β*-AD study was launched in 2022 to provide a methodology based on the combination of Monte-Carlo codes and active neutron detectors to assess activation inside materials of cyclotron facilities: neutron fluences calculated with Monte-Carlo codes will be validated by measurements made with active autonomous miniaturised CMOS detectors and will be applied to assess activation of materials and definition of ratio between *β*-only and *γ*-emitting radionuclides.

First experiments were conducted in 2021 at the Cyclotron CEMHTI facility, a multi-beam (protons, *α*, deuterons), multi-intensity (15 µA to 40 µA) and multi-energy (5 MeV to 50 MeV) accelerator used for radionuclides productions [1], irradiation experiments [2], neutrontherapy [3]. First beams were delivered in 1976 until its shut-down in 2023. The goal of these first experiments is to benchmark Monte-Carlo codes with experimental setup in an existing facility to identify possible differences or discrepancies depending on the codes.

Passive activation foils of different materials were placed inside experimental vaults during two kinds of irradiations with main beam parameters used in the last years of operations (protons and deuteron beam). *γ*-spectroscopy was made on the samples at the end of irradiation. Results were then compared with calculations made using different Monte-Carlo codes: FLUKA [4, 5], MCNP6 [6], PHITS [7] and RayXpert [8, 9].

1 Models

The aim of the study is to compare activation assessed by Monte-Carlo codes with experimental measurements on activation foils irradiated by CEMHTI Cyclotron during operation for two different beams: protons inside the bunker and deuterons inside one of the experimental areas. Relevant parts

that could impact the production of secondary particles are modelled with a high accuracy, based on blueprints provided by CEMHTI team: magnets, targets, yoke and radiological protections. Monte-Carlo codes are set up to improve the statistics regarding the neutron production.

1.1 Geometrical Model

1.1.1 Bunker and experimental areas

A complete bunker and experimental areas building model is made as accurate plans (provided by CEMHTI team and based on some data from the original builder) are available (Fig. 1–2).

Various versions of the cyclotron vault and the transport beam line were implemented to add relevant parts: vacuum chamber surrounding the target, biological protections around the target made of light concrete (d = 0,56) and magnets upstream and downstream the target (Fig. 3).

A basic composition of heavy concrete, based on database from Flair [10], was used.

1.1.2 Cyclotron

Cyclotron model is based on partial blueprint of the accelerator and *in-situ* measurements. Main parts for the secondary particles production are the yoke surrounding the vacuum chamber where ion beam is accelerated and the top and bottom magnets. Inside the vacuum chamber, the inflector is accurately modelled as this part is used to simulate beam losses.

1.1.3 Targets

Targets for each of both different beams are modelled based on information provided by the CEMHTI team. For protons, primary beam is stopped in a block of tantalum target (7.0 × 7.0 × 5.6 cm). For deuterons, primary beam is stopped inside a cylindrical beryllium target (diam.=5 cm, width = 0.5 cm).

1.2 Physics settings

1.2.1 Beam losses

For proton beam, two locations are defined as beam losses: the main one is the tantalum target (beam impeding directly on the block), the second one is a partial loss of primary beam on the start of the deflector (Table 1). The size of the beam or the energy spread is not implemented in this study.

For deuteron, the whole beam is lost inside the beryllium target with the parameters described in Table 1.

Table 1
Parameters for protons and deuterons beam

Parameters	Value	
Particle	Protons	Deuterons
Energy	16 MeV	17.5 MeV
Intensity on Beam-Stopper	25 µA	-
Intensity on deflector	5.75 µA	-
Intensity on Be target	-	30 µA
Size	Pencil beam	

1.2.2 Monte-Carlo codes settings

The same geometrical model, with same materials and beam parameters are implemented in the different Monte-Carlo codes used. Some specifics settings are defined for each code to improve results.

FLUKA Physics parameters are based on the PRECISIO card. Activation calculations are made using on-line capabilities of the code. Last versions implemented point-wise cross sections for neutrons reactions and deuteron interaction physics that had been used. Different libraries or models are used to handle the interaction for neutrons, protons and deuterons:

- Neutrons: JEFF 3.3 [11]
- Protons: interaction handled with the PEANUT module (for the energy considered) and FLUKA Multiple Coulomb Scattering model
- Deuterons: Boltzmann-Master Equation and RQMD [12]

The steps for transport of electromagnetic particles, hadrons and muons are reduced for all materials, excepted air, by a factor of 0.05 for electromagnetic particles and 0.01 for hadrons/muons. Survival probability for neutrons with energy lower than 20 MeV are fixed to 95%, inelastic nuclear interaction length is reduced by a factor of 40 in all the materials (excepted air) to improve the production of neutrons. Importance variance reduction is applied to activation foils with a factor of 5. To reduce the computing time, photons production and transport energy threshold are defined to 8 MeV.

MCNP6 MCNP6.3 version is used in the present study. TENDL-2021 [13] libraries are used for neutron and photonuclear reactions, and TENDL-2019 for proton and deuteron interactions. Default settings for neutron physics are used. For photons, maximum energy for the detailed physics treatments was 25 MeV and photonuclear interactions are activated, otherwise default settings are used. For protons and deuterons, the maximum energy for transport and production is set to 80 MeV, light ions recoil is activated (with production of one light ions at each proton scatter event with light nuclei), otherwise default settings are used. Forced collision on activation foils is used as variance reduction technique for neutrons and photons.

PHITS TENDL-2021 libraries are used for neutron, proton and photonuclear reactions. Forced collisions are used for activation foils region. JMQD-2.0 model [14] is used for nuclear reactions. Otherwise, defaults settings are used.

RayXpert By default, the ENDF/B-VIII.0 [15] cross sections library is used for neutron transport in RayXpertV2.0.1. Nevertheless, several cross sections libraries are available in RayXpert: ENDFB-VII.1 [16], JEFF3.3, JEFF3.1 [17] and TENDL2024.

To be aligned with the others computation software involved in this study, the neutrons flux computations in RayXpert have been performed with the TENDL2024 database. For proton transport, the physic list used is QBBC [18]. The energy range covered by this physic list is up to 10 TeV, which covers the energy domain required for this study. The secondary particle thresholds for electrons, positrons and photons are set to 100 keV. No other variance reduction technique is used. For the flux computations, the Monte Carlo estimator “track” is used.

2 Experimental Settings

Activation foils of different materials were irradiated during monitored runs. *γ*-spectroscopy was made to assess the activity of *γ*-emitter radionuclides and results are compared with calculations made with numerical simulations.

2.1 Activation Foils

Activation foils of different materials were placed inside a room where neutron fluence needs to be characterized. This protocol is widely used for particle accelerators and cyclotrons [19–22]. The choice of the materials is based on the following criteria:

- Only one stable nucleus naturally available to reduce the number of pathways.
- Distinct resonance region for the reaction cross-section with thermal neutrons (n,*γ*) to cover a large range of low energy neutrons.
- Different energy threshold for (n,p)/(n,2n) reactions.
- Materials available as foils and with high purity to reduce creation of impurities.
- Radionuclides produced with half-life compatible with *γ* spectroscopy measurements and radiation protection (access to irradiation room, handling…).

Four materials were chosen: Au, Sc, Ta and Tb. Standard dimensions (excluding width) were used for the foils: 2.5 × 2.5 cm. Width depends on the materials and the references available from the providers (Au, Tb: 1 mm, Sc: 0.5 mm, Ta: 2 mm). One activation foil of each material was placed at each irradiation location as a 2*2 matrix.

Proton beam Activation foils were placed inside the cyclotron vault at different locations (Fig. 4). A 25 µA-16 MeV proton beam were stopped in the tantalum block during 5 h.

Deuteron beam Activation foils were placed inside the experimental aeras at different locations (Fig. 5). A 30 µA-17.5 MeV/A deuteron beam were stopped in the beryllium target during 2 h

Two batches of irradiations were conducted in 2021. Sc, Ta and Tb foils used during the first batch were re-used in the second batch to reduce the environmental impact and to check the effect of multiple irradiations and cooling time in results obtained. Locations of the different matrixes of activation foils depending on the primary beam is described on Table 2.

Table 2
Different settings and locations of the activation foils for both batches of irradiation

Beam	Date	Activation Foils used				
h		Extraction	Pipe	Yoke	Deflector	Wall
	03/2021	Sc/Ta/Tb				
	10/2021	Au/Sc/Ta/Tb				
d		Wall	Door	Magnet		
	03/2021	Sc/Ta/Tb				
	10/2021	Au/Sc/Ta/Tb				

2.2 *γ*-spectroscopy

A 40% -efficiency ISOCS characterized detector was used for the *γ* spectroscopy of activation foils. Each activation foil was measured during 5000 s (active time). Distance between sample and detectors are the same for each activation foil (d = 2.5 cm). ISOCS [23] was used to calculate the efficiency regarding the geometry of the sample. “Rectangular plane” template was chosen. Uncertainties were evaluated using the tools provided in the software.

3 Results

Activation produced in the samples is calculated using neutron fluences produced by the Monte-Carlo codes. With FLUKA, on-line activations calculations are performed using irradiations parameters. For the all the codes, off-line activation calculations are performed using FISPACT-II [24] with TENDL-2019 as neutron cross-sections library and RayActive with MCNP6 neutron fluences.

RayActive is a software dedicated to the simulation of residual dose induced by neutron activation. It is based on the R2S method, standing for Rigorous Two Steps, which combines neutron transport calculations using the Monte Carlo method, the evaluation of activation-induced isotopic inventories, and the subsequent simulation of radiation emitted during radioactive decay. The software relies on CAD-based geometry, enabling accurate modelling of complex industrial or experimental systems.

Monte Carlo calculations are performed using RayXpert, which is also used to simulate radioactive decay and the transport of the associated secondary radiation. RayActive provides several ordinary differential equation solvers for isotopic inventory calculations: one solver based on a BDF method [25] and several solvers based on Block BDF methods, offering increased stability for solving the Bateman equations.

The software can perform a complete activation calculation, from neutron flux evaluation to residual dose calculation, while also allowing each step of the method to be run independently. It also provides the capability to perform standalone isotopic inventory calculations. Finally, a specific optimization has reduced memory consumption during neutron transport by sharing detectors among the different computational threads, without any significant loss of performance.

3.1 Proton beam

Results from both campaigns are used to compare measurements and calculations (Table 3 and Fig. 6).

Table 3
Activity measured by *γ*-spectroscopy during proton irradiation campaigns (03/2021 and 10/2021) for each activation foils

Location	Radionuclides	Activity (Bq)
Extraction	198Au	(5.4 ± 0.6) × 104
	46Sc	(9.7 ± 0.5) × 101
	182Ta	(10.0 ± 0.2) × 102
	160Tb	(6.2 ± 0.1) × 102
Pipe	198Au	(1.1 ± 0.1) × 105
	46Sc	(2.6 ± 0.1) × 102
	182Ta	(2.4 ± 0.5) × 103
	160Tb	(1.9 ± 0.3) × 103
Yoke	198Au	(2.1 ± 0.2) × 104
	46Sc	(4.3 ± 0.2) × 101
	182Ta	(3.0 ± 0.9) × 102
	160Tb	(2.3 ± 0.6) × 102
Deflector	198Au	(1.3 ± 0.1) × 104
	46Sc	(2.6 ± 0.1) × 101
	182Ta	(1.8 ± 0.5) × 102
	160Tb	(1.4 ± 0.4) × 102
Wall	198 Au	(1.0 ± 0.1) × 104
	46Sc	(2.2 ± 0.1) × 101
	182Ta	(1.3 ± 0.4) × 102
	160Tb	(8.0 ± 0.3) × 101

Ta, Tb and Au show higher differences between codes with activation foils located next to a beam loss point (“deflector” and “pipe”). Due to their higher sensitivity with low-energy neutrons compared to Sc, this behaviour could be related to differences of low-energy neutron fluences calculations with small angles between codes. In the other hand, for foils not located next to a beam-loss point the trend of the different codes is similar.

FLUKA on-line calculations results are in good agreement with measurements except for Au. Differences come from the use of an arbitrary 50%-50% ratio between ground state and isomer radionuclides when

using RESNUCLEI. These results are improved using FISPACT-II (this issue can be addressed by using USRYIELD card too in FLUKA).

PHITS shows trend like FLUKA in most cases, in the other hand RayXpert shows trends like MCNP6.

Despite uncertainties around the intensity of beam losses on each point, it must be noted that the results are in the expected range of performance. Improvements could be made by a better knowledge of the beam parameters like intensity loss or its shape for instance.

3.2 Deuteron beam

Comparison between measurements and calculations shows good agreement using FISPACT with neutron fluences produced by FLUKA, MCNP6 and PHITS (Fig. 7).

Table 4
Activity measured by *γ*-spectroscopy during deuteron irradiation campaigns (03/2021 and 10/2021) for each activation foils

Location	Radionuclides	Activity (Bq)
Wall	198Au	(6.8 ± 0.7) × 105
	46Sc	(1.2 ± 0.6) × 103
	182Ta	(7.1 ± 0.1) × 103
	160Tb	(4.2 ± 0.7) × 103
Door	198Au	(5.4 ± 0.6) × 105
	46Sc	(1.1 ± 0.6) × 103
	182Ta	(5.6 ± 0.1) × 103
	160Tb	(3.4 ± 0.6) × 103
Magnet	198Au	(2.9 ± 0.3) × 105
	46Sc	(5.0 ± 0.2) × 102
	182Ta	(2.9 ± 0.6) × 103
	160Tb	(2.0 ± 0.3) × 103

Results from on-line calculations with FLUKA are always very underestimated with Au foils due to the same issues explained in the previous subsection. In other cases, results from calculations are mostly overestimated, leading to an overestimation of low-energy neutron produced with the reaction Be(d,n) and the thermalisation on wall concrete.

Nevertheless, results from Monte-Carlo codes coupled with FISPACT-II are in the expected range.

4 Conclusion

This study shows that neutron fluences estimation from Monte-Carlo code, with a relatively accurate model, give good agreement for activation assessment of passive detectors, within a range of 0.5–1.5 between measurement and calculation. The main source of uncertainty for proton beam comes from the lack of accurate information regarding the intensity of losses in the accelerator. FLUKA on-line calculations, despite some issues to handle isomer equilibrium, give good results for proton and deuteron beam. RayXpert, FLUKA, MCNP6 and PHITS neutron fluences used with FISPACT-II and TENDL19 or TENDL21 neutron, proton or deuteron cross-section libraries are in good agreements with experiments, with a trend to overestimate activation. RayXpert and MCNP6 shows similar behaviour with higher discrepancies with other codes next to the beam-loss points, mainly due to the underestimation of low-energy neutron fluence in small angles with the proton beam. Based on the results obtained, two new studies are made in the frame of the Simβ-AD study to determine specific differences between Monte-Carlo codes and cross-section libraries: neutron production on simplified models and behaviours regarding the target and the scattering angles, and another one regarding neutron thermalization with concrete.

As the CEMHTI cyclotron is now shut-down, new studies will be made to compare numerical simulations results with measurements made on different parts of the cyclotron and on the wall concrete of the vault or the experimental areas.

Declarations

Declarations

This work was granted access to the HPC resources of IDRIS under the allocation AD011015560R1 made by GENCI.

This work was supported by Bpifrance (DOS0197398/00) and the French government in the frame of FRANCE 2030 - Financed by European Union - Next Generation EU, in the frame of the France Relance plan.

Author Contribution

JMH wrote the main manuscript text and realise acquisition, analysis, or interpretation of data.AH helps to the analysis, interpretation of data and revised the manuscript criticallyFC helps to realise acquisition of dataNA realises interpretation of data and revised the manuscript criticallyLN-CD realise analysis, interpretation of data and revised the manuscript criticallyDB-LVGG-SH-SB-DC-WH-PR-TS help to realise acquisition of dataJMH-AH-FC-NA-LN-CD-DB-LVGG-SH-SB-DC-WH-PR-TS reviewed the manuscript and approved the version to be published

Acknowledgments

I want to thank all the CEMHTI Cyclotron team for their help and to give me the opportunity to realize this experiments, especially Thierry Sauvage to provide beam time for the Sim*β*-AD study. Thanks to Dominique Baux, Arno Gainville, William Hate, Paul Sigot for their help. A special thanks to Patrice Rifard, providing me with extremely valuable information about the cyclotron and for all our discussions. And a very special thanks for the Radiation Protection team, Sebastien Bouillon and David Chaulin, for their help and their enthusiasm.

References

1. Malikidogo KP et al (2018) A cocktail of 165Er(iii) and Gd(iii) complexes for quantitative detection of zinc using SPECT and MRI. Chem Commun 54(55):7597–7600
2. Beauchesne F, Barrandon JN (1986) Analyse globale et non destructive des objets archéologiques cuivreux par activation avec des neutrons rapides de cyclotron. Revue d'Archéométrie 10(1):75–75
3. Sabattier R, Destembert N, Fau - B, Breteau, Breteau N Tech status Rep Orleans neutron therapy facility. (0179–7158 (Print)).
4. Ahdida C et al (2022) New Capabilities of the FLUKA Multi-Purpose Code. Frontiers in Physics, p 9
5. Battistoni G et al (2015) Overview of the FLUKA code. Ann Nucl Energy 82:10–18
6. Kulesza JAaA, Terry R, Armstrong JC, Bolding SR, Brown FB, Bull JS, Burke, Timothy Patrick and Clark, Alexander Rich and Forster, III, Robert Arthur and Giron, Jesse Frank and Grieve, Tristan Sumner and Josey, Colin James and Martz, Roger Lee and McKinney, Gregg Walter and Pearson, Eric J. and, Rising (2022) Michael Evan and Solomon, Jr., Clell Jeffrey and Swaminarayan, Sriram and Trahan, Travis John and Wilson, Stephen Christian and Zukaitis, Anthony J., *{MCNPextsuperscript{extregistered} Code Version 6.3.0 Theory \& User Manual}*. Los Alamos National Laboratory
7. Sato T et al (2024) Recent improvements of the particle and heavy ion transport code system – PHITS version 3.33. J Nucl Sci Technol 61(1):127–135
8. Dossat C (2026) RayXpert: User Guide. TRAD
9. Dray N et al (2024) An overview of last decade's developments in RayXpert®, a 3D Monte Carlo code. EPJ - Nuclear Sciences & Technologies, p 10
10. Donadon A et al (2024) FLAIR3 – recasting simulation experiences with the Advanced Interface for FLUKA and other Monte Carlo codes. EPJ Web Conf., p 302
11. Plompen AJM et al (2020) The joint evaluated fission and fusion nuclear data library, JEFF-3.3. Eur Phys J A 56(7):181
12. Andersen V et al (2004) The FLUKA code for space applications: recent developments. Adv Space Res 34(6):1302–1310

13. Koning AJ et al (2019) TENDL: Complete Nuclear Data Library for Innovative Nuclear Science and Technology. Nucl Data Sheets 155:1–55
14. Ogawa T et al (2015) Energy-dependent fragmentation cross sections of relativistic $^{12}\mathrm{C}$. Phys Rev C 92(2):024614
15. Brown DA et al (2018) ENDF/B-VIII.0: The 8th Major Release of the Nuclear Reaction Data Library with CIELO-project Cross Sections, New Standards and Thermal Scattering Data. Nucl Data Sheets 148:1–142
16. Chadwick MB et al (2011) ENDF/B-VII.1 Nuclear Data for Science and Technology: Cross Sections, Covariances, Fission Product Yields and Decay Data. Nucl Data Sheets 112(12):2887–2996
17. Santamarina A et al (2009) The JEFF-3.1. 1 nuclear data library. JEFF Rep 22(102):2
18. Ribon A et al (2010) *Status of GEANT4 hadronic physics for the simulation of LHC experiments at the start of LHC physics program.* CERN-LCGAPP, 2: p. 2010
19. Jo J et al (2018) Initial result of neutron energy spectrum reconstruction using multi-foil activation method in KSTAR. Fusion Eng Des 136:793–796
20. Judd AM (1963) Neutron flux measurements by resonance activation of foils. Nucl Instrum Methods 23:29–35
21. Lengar I et al (2018) Activation material selection for multiple foil activation detectors in JET TT campaign. Fusion Eng Des 136:988–992
22. Nobuhara F et al (2017) Neutron transport calculation for Activation Evaluation for Decommissioning of PET cyclotron Facility. EPJ Web Conf, p 153
23. Venkataraman R et al (2005) Improved detector response characterization method in ISOCS and LabSOCS. J Radioanal Nucl Chem 264(1):213–219
24. Sublet JC et al (2017) FISPACT-II: An Advanced Simulation System for Activation, Transmutation and Material Modelling. Nucl Data Sheets 139:77–137
25. Curtiss CF, Hirschfelder JO (1952) Integration of Stiff Equations. Proc Natl Acad Sci U S A 38(3):235–243

Figures

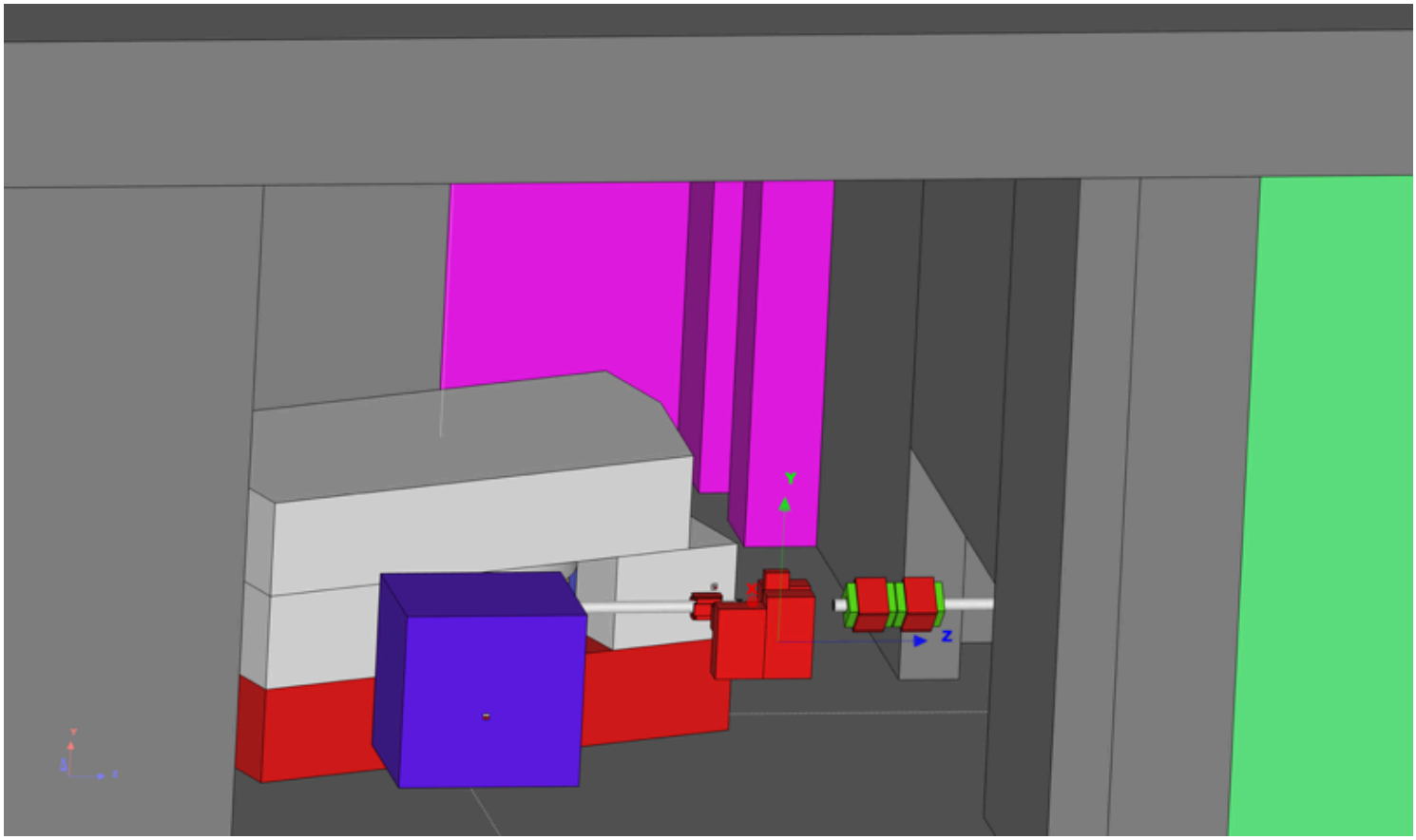


Figure 1

View of the bunker and experimental areas of the CEMHTI Cyclotron facility produced with RayXpert

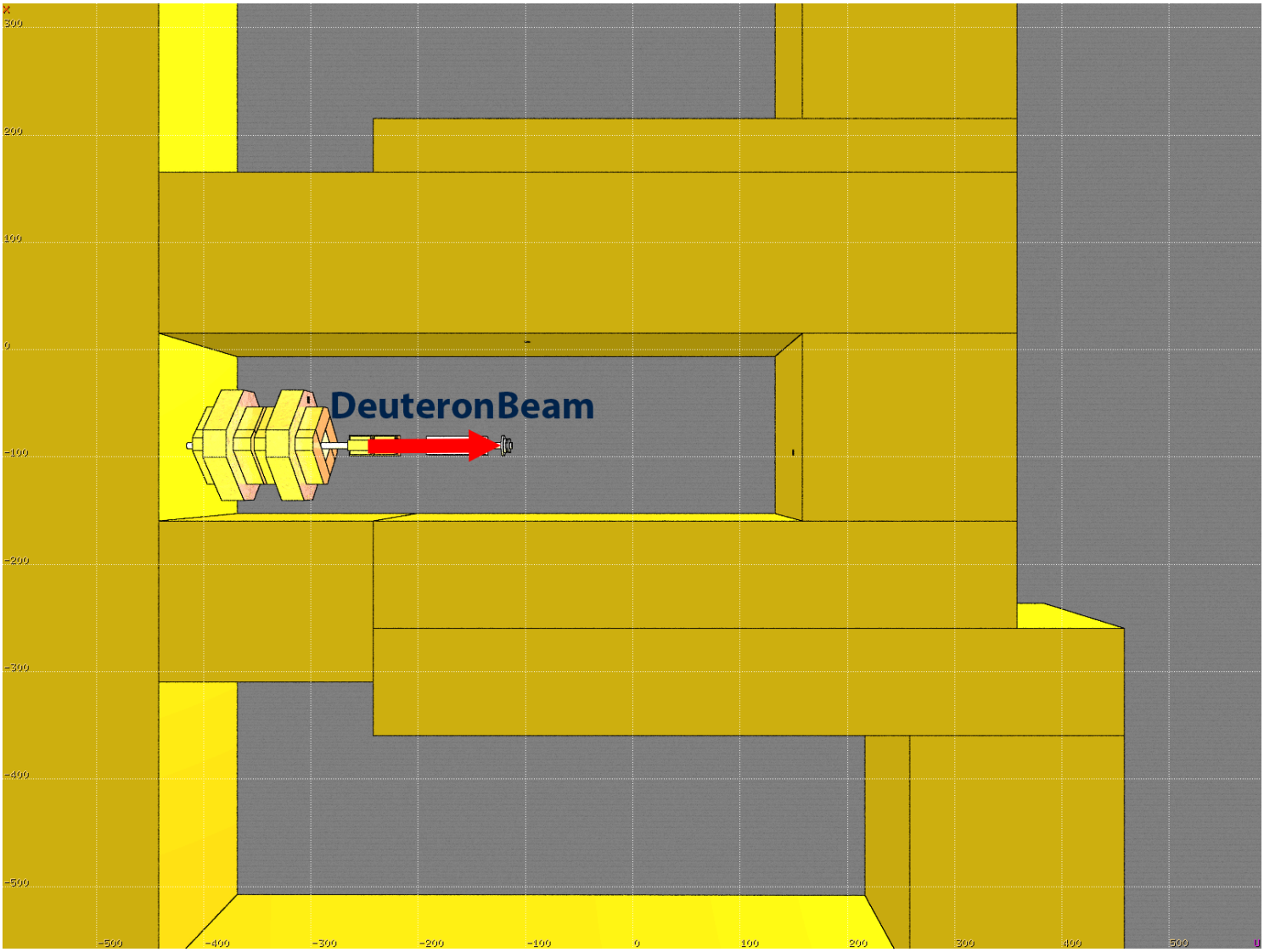


Figure 2

Top view of the experimental area with set-up for irradiation with neutron beam produced with deuteron primary beam on a Be target produced with FLAIR

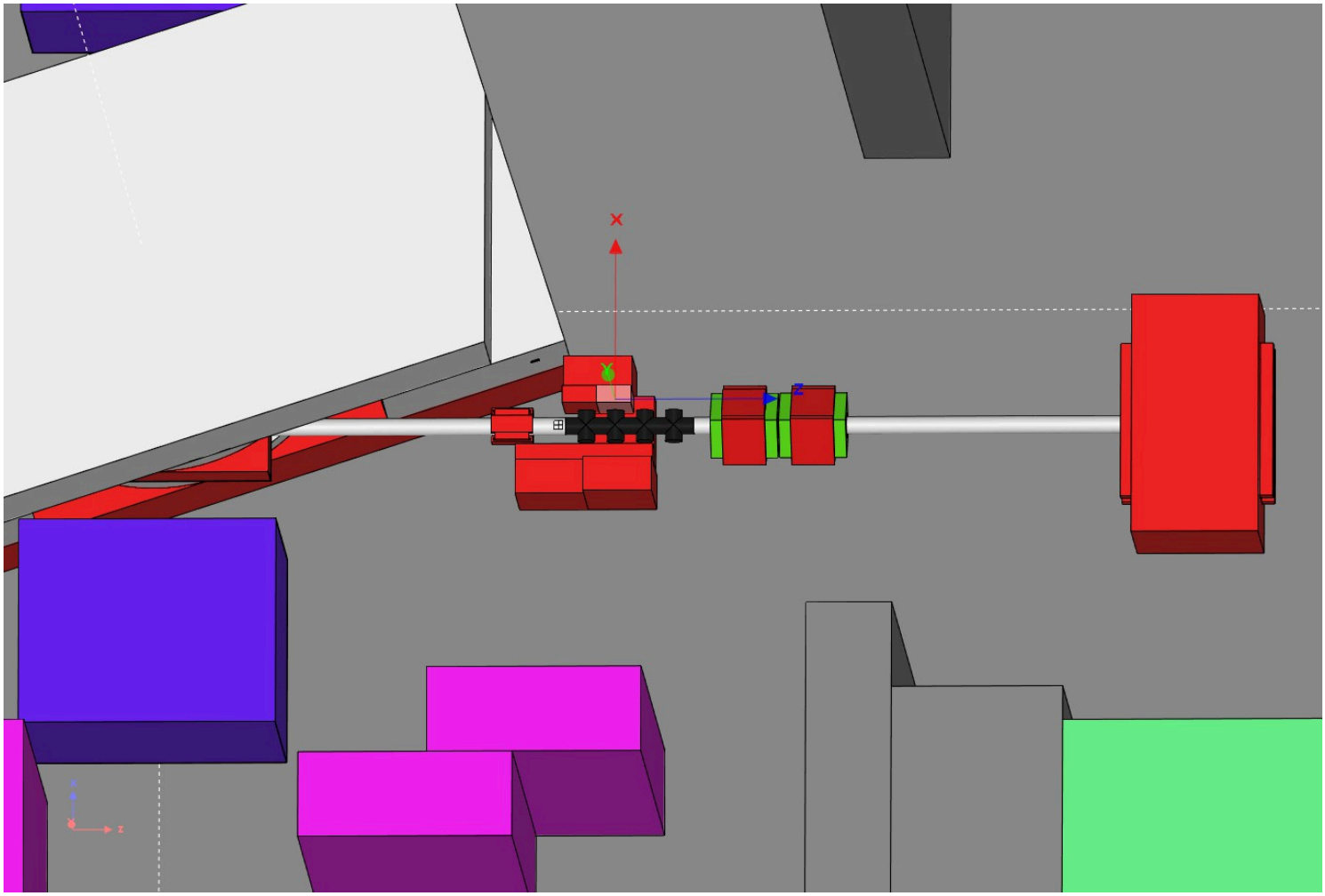


Figure 3

Top view of the extraction beam line of the CEMHTI cyclotron with magnets, vacuum chambers, targets and biological protections produced with RayXpert

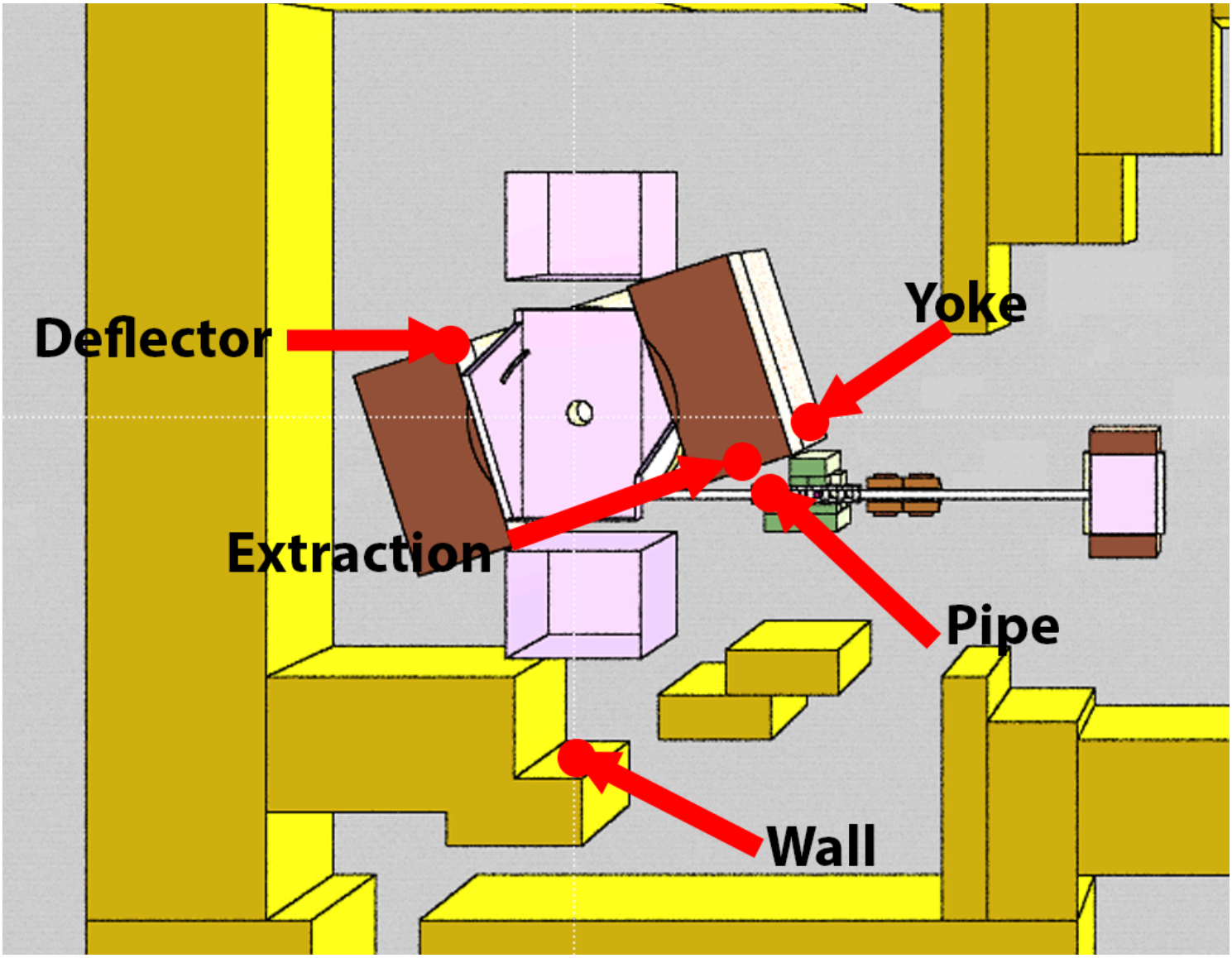


Figure 4

Location of the activation foils during proton beam irradiations

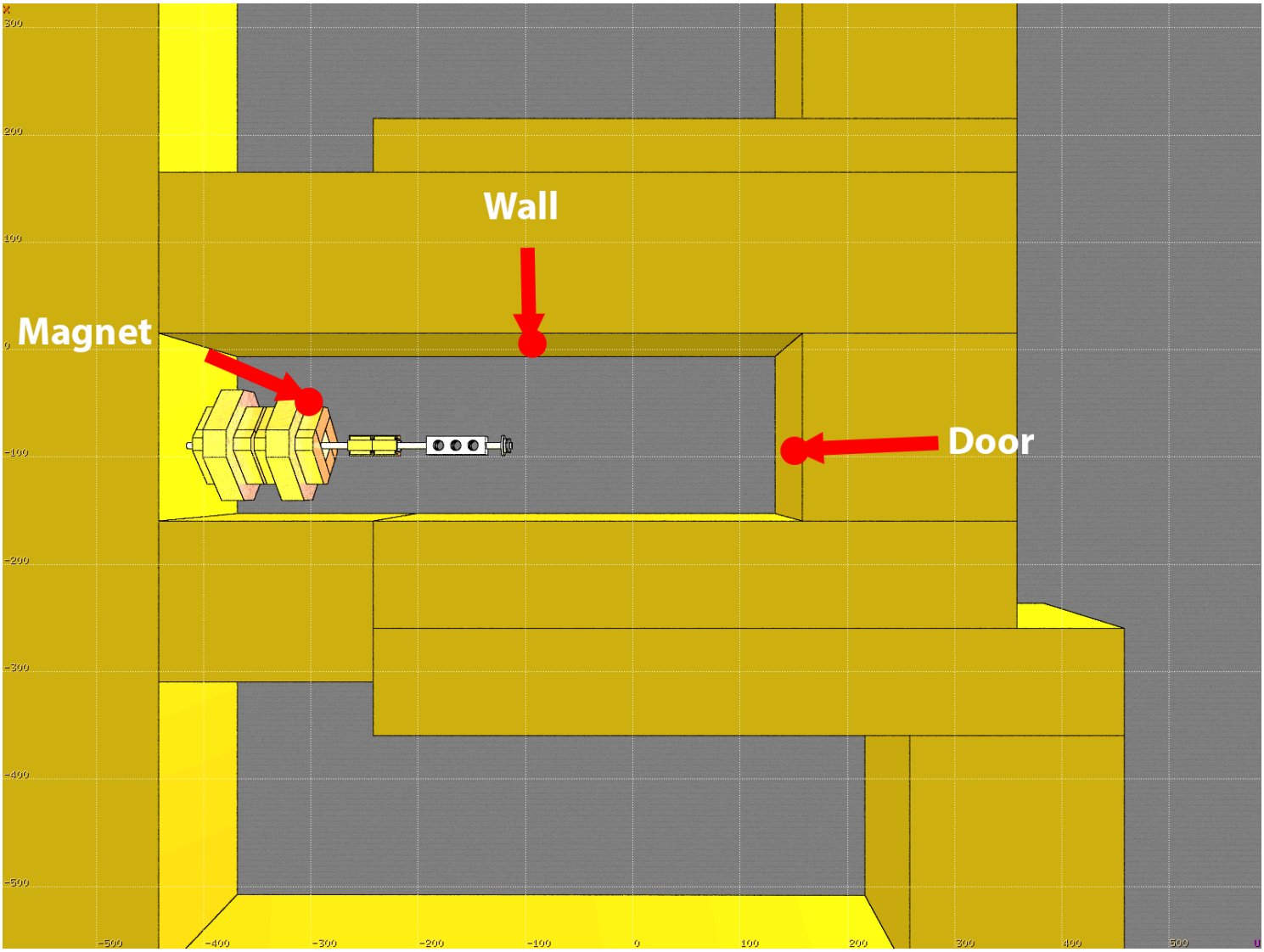


Figure 5

Location of the activation foils during deuteron beam irradiations

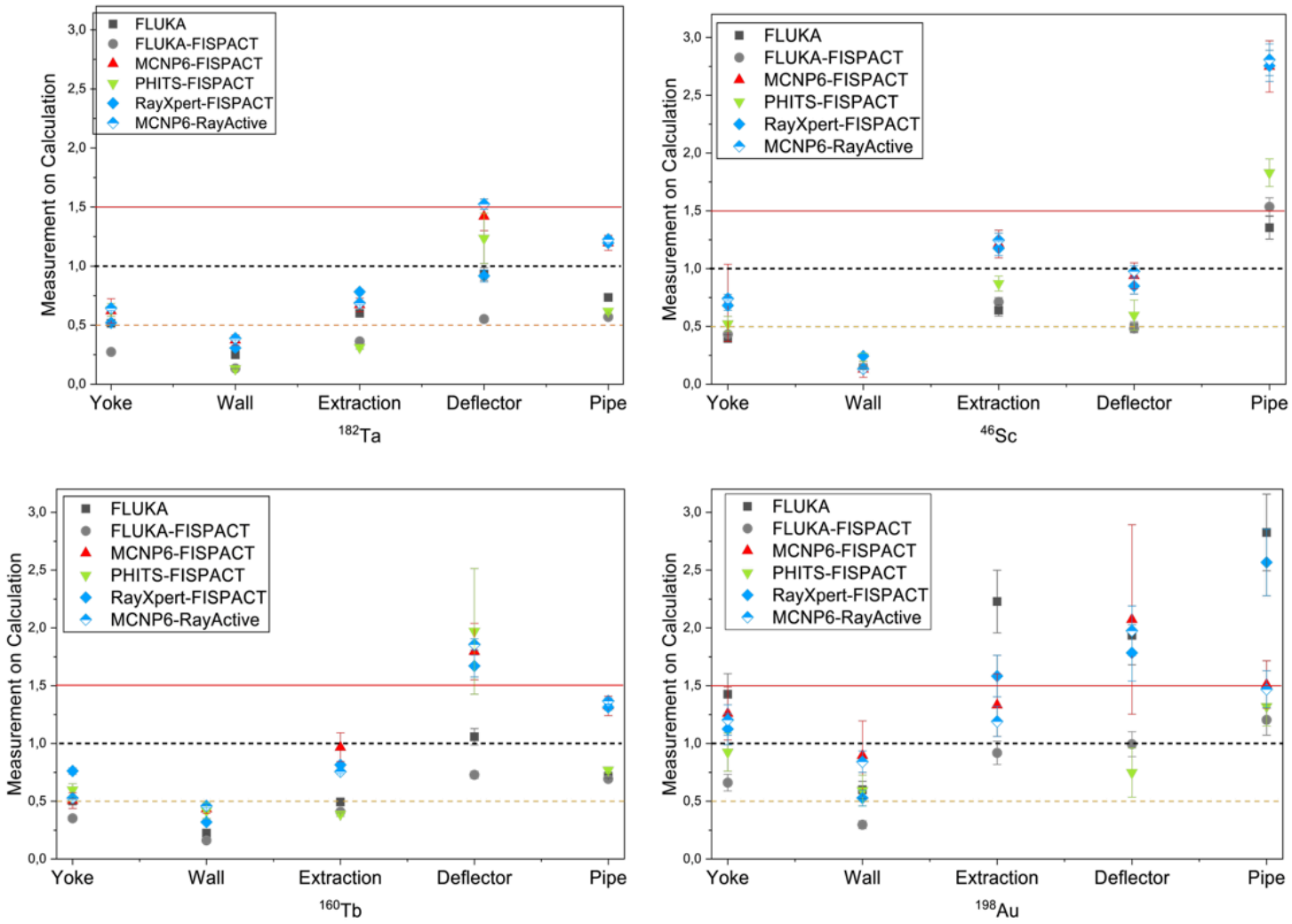


Figure 6

Ratio measurement on calculation for the different activation foils irradiated with proton beam for both irradiation campaigns

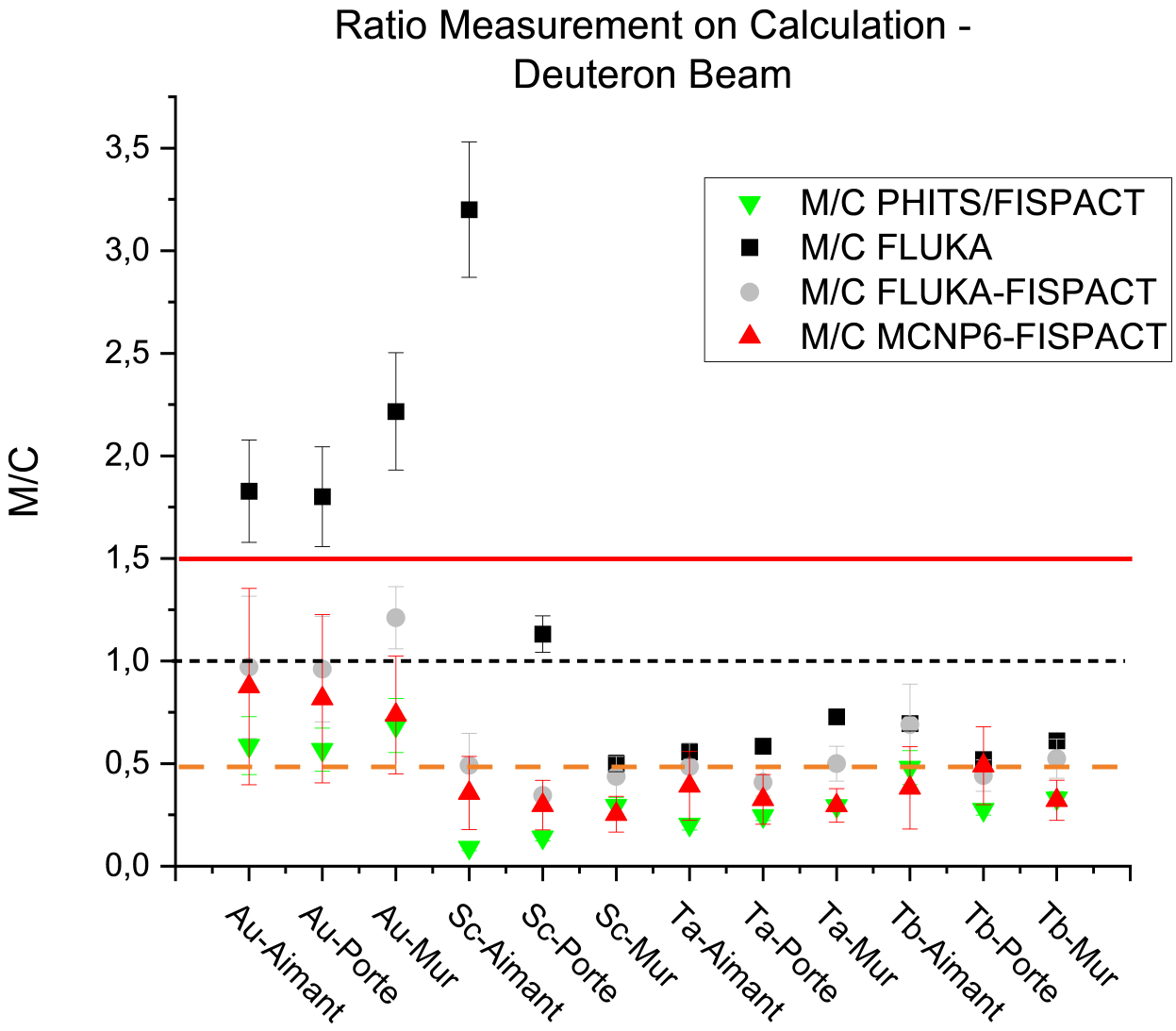


Figure 7

Ratio measurement on calculations for the different activation foils irradiated with deuteron beam for both irradiation campaigns